SYMBIOTIC AND OPTIMIZED ENERGY SUPPLY FOR DECARBONIZING CHEESE PRODUCTION: AN ITALIAN CASE STUDY

D.Chinese[1*], P.F. Orrù[2], G. Cortella[1], A. Meneghetti[1], L. Giordano[3], M. Benedetti[3]

1. DPIA, Polytechnic Department of Engineering and Architecture, University of Udine, Udine, Italy; email: damiana.chinese@uniud.it
2. DIMCM, Department of Mechanical, Chemical and Materials Engineering, University of Cagliari, Cagliari, Italy
3. ENEA, Italian National Agency for New Technologies Energy and Sustainable Economic Development, Rome, Italy

ABSTRACT

The use of renewable energy, including solar process heating, and of efficient energy conversion technologies, have been considered in the literature to improve the energy performance of cheese production. However, most of the studies consider one energy source at a time, or hardly account for the carbon emission impact of different energy supply alternatives. Furthermore, the role of symbiotic options such as recovering waste heat from remote industrial processes to meet the significant thermal energy demand of cheese factories is hardly explored. In this paper, a mixed integer linear programming model is developed and applied to a reference cheese factory in Italy to identify the least cost mix of industrial waste heat, solar process heating and natural gas-based trigeneration which allows to achieve assigned carbon emission reduction goals. It is found that, at current economic conditions, fossil fuel based trigeneration is economically attractive but does not contribute to decarbonization, whereas a combination of cogeneration and waste heat recovery from a remote source may be more efficient than solar heating in achieving decarbonization goals at a lower cost.

Keywords: Energy supply, dairy industry, waste heat recovery, decarbonization, trigeneration

1 INTRODUCTION

In a worldwide context of increasing overall global dairy production, Italy plays a major role particularly in the cheese sector. In Italy, about 13 million tons of milk are converted yearly into one million tons of cheeses, and about one quarter of those is exported.

However, dairy products are among the most impactful food products, particularly as to their carbon footprint [1]. Scientific literature [2] confirms that both carbon emissions and fossil fuel consumption are mainly caused by raw milk production, including dairy farming and cultivation of feed crops, but industrial processing of milk is the second largest determinant of greenhouse gas emissions. In fact, in dairy industries significant energy amounts are spent for milk pasteurization and heating, on one hand, and for refrigeration,

on the other [3]. In fact, depending on cheese type and maturation the values of specific electric energy consumption for cheese production from raw milk reported in the literature can vary in a range of 0.2 [4][5] to almost 3 kWh/kg of final product [2], and specific thermal energy consumption is reported to vary from 0.1 [4] to almost 8 MJ/kg [2] of final product, where values at lower ends of ranges are generally reported for soft cheeses with short ripening and high water content.

Given the energy intensity of cheese production, several researchers have focused on improving the energy efficiency of dairy industries and on enhancing the use of renewable energy in milk transformation processes.

As to renewable energy, a solar field has been proposed to meet the heating demand of a cheese and yoghurt factory in Spain [6], while a cascade of solar systems has been designed to supply process heat to a milk drink factory in Morocco [7]. Pilot projects also include milk pasteurisation, which in many countries is a mandatory treatment of milk for cheese production, performed at temperatures up to 70°C with solar energy using flat or evacuated solar panels [8]. Biomass is also considered in many studies, either as a generic option for electricity generation [9] or as well identified bioproducts or waste products from the dairy and the food industry, which can be integrated in circular economy [5] and biorefinery concepts [10] with the use of biological treatments, mainly of anaerobic digestion [11][12].

As to energy efficiency, fossil fuel based polygeneration, that is, the simultaneous production of two or more energy services or products that use process integration schemes to achieve higher energy utilization [13] has recently been investigated in [14] for a milk processing industry in Southern Brazil. Based on a systematic review, the authors of [5] observed that no studies on the optimization of polygeneration systems dealing with the dairy industry were available, and they introduced a mixed integer linear programming model to optimize the size and operation of combined heat and power generation technologies, also including biomass boilers and absorption cooling systems among the technologies under consideration. However, while giving a full account of the economic benefits of cogeneration, they do not account for the environmental impact of different design choices. Furthermore, based on our brief review of the literature, hybrid polygeneration systems including e.g., a combination of cogeneration and solar heating are hardly considered for the dairy industry, although there are some examples for farming [15].

Industrial symbiosis, that is the connection of industries by exchanging unused/wasted by-products [16], can be declined as industrial energy symbiosis [17][18] if energy flows are the main by-products exchanged between different industries. This is the case of the external use of excess heat, which can be transferred from the waste heat generating company to a potential user by means of a district heating infrastructure. Literature [18]-[20] shows that the input of excess heat from industries in existing district heating networks supplying urban areas and residential buildings is much more frequent than purely industrial energy symbiosis, which mainly happens in eco-industrial parks where many large companies are located [21], as well as than the construction of new and dedicated district heating infrastructure.

Nevertheless, a recent work [22] has also demonstrated that point-to-point district energy infrastructure connecting industrial companies discarding excess heat to the environment to large scale residential users is economically viable even at relatively small scales and large distances (e.g a 10 km district heat pipe of 10 MWth capacity connecting residential users with a matching peak demand would be feasible under Austrian climatic conditions) and always brings about benefits as to carbon emission reduction. We can infer that point-to-point delivery of industrial waste heat would be also feasible at a smaller scale within industrial areas or districts, particularly for industries requiring high and steady flows of low-grade heat for process purposes. Starting from point-to-point connections, solutions can then be replicated at a district level, reaping economies of scale and scope to build larger systems [23].

As this is the case in the dairy industry, particularly for cheese production, the use of excess heat from other industries located in the same area could be an interesting option for this sector. On the other hand, it can be expected that if cost efficient and low carbon technologies are available to meet heating demand, they may jeopardize the financial viability of polygeneration approaches, which relies on a steady heating demand as well.

This paper aims to explore this kind of interaction for the dairy industry by analysing a realistic case study of a reference cheesemaking plant in the Italian context, which is described in section 2.

Optimization based on mixed integer linear programming is a state-of-the-art methodology not only, as demonstrated in [14], for the design of polygeneration systems, but also for the design of district heating systems, particularly to identify an optimized design and operation of infrastructure and of the related energy conversion equipment at the same time [24]. Several authors [25]-[27] have introduced mixed integer linear programming models to support the design of industrial polygeneration systems integrated with district heating: however, most examples focus on optimizing the management and sale of excess heat from a polygenerating company to a district energy grid, and just a few [28] evaluate the efficiency of being supplied with district heat from different sources as compared with cogeneration or alternative energy conversion options.

On this background, this paper aims to fill this gap by adapting and expanding the optimization model introduced for a Brazilian dairy industry by [14], as described in section 3, so that external excess heat supply and solar energy supply are considered and integrated as additional options for decarbonizing milk processing operations. An additional element which has been added to the original model [14] are carbon footprint constraints, which allow to evaluate alternative configurations also under this respect. The results of the model application to the selected case study are presented and discussed in section 4.

2 CHEESE PRODUCTION: CASE STUDY DESCRIPTION AND ENERGY PROFILES

A Sardinian cheese factory was taken as a reference plant, which processes yearly about 8,6 Ml of sheep and goat milk. More than 60% of the raw milk goes to the production of semi-hard and mature cheese, and the

remaining quantity is used for soft cheese. The production process is like the one described in [2] for a medium-large industry, although a wider variety of products is processed in the present case. An energy audit of the plant was performed, by identifying and modelling the process energy loads and their time profiles. As in the case of [3], pasteurization is performed daily from 08:00 h to 13:00 h and requires high temperature (95°C) water. Hot water is also required for cleaning and for producing ricotta: the whey is heated up to about 80 °C to induce the denaturation and precipitation of whey proteins, which are then filtered to separate the solid part (ricotta cheese). On the other hand, lower temperature hot water, at less than 70°C, is required for maintaining operations and ripening cells at constant and controlled conditions (mainly at 12°C and 50% humidity) and for plant basic operations. Through the energy audit, heat load profiles were derived for both low and high temperature heating processes by combining thermodynamic models of cells and heat exchanges with the monitoring of processed milk quantities. Models were validated by comparison with monthly fuel demand observed at the plant. Table 1 depicts the average daily flow required by the cheesemaking process for typical days of each month, as well as yearly average values.

	HT Heat demand [kW]	LT Heat demand [kW]	Cooling demand [kW]	Power demand [kWe]
January	96.1	196.5	202.1	305.2
February	104.8	222.8	233.2	305.7
March	115.9	238.7	255.5	370.4
April	117.4	252.9	276.9	385.8
May	108.7	248.9	275.3	379.5
June	88.5	225.0	255.2	390.3
July	70.0	180.7	225.0	349.6
August	57.5	154.6	201.1	351.8
September	45.5	60.5	111.0	342.8
October	45.5	60.5	111.0	281.2
November	47.5	56.0	72.1	241.0
December	72.6	159.3	156.3	230.4
Yearly AVG	*80.8*	*171.4*	*197.9*	*327.8*

Table 1. Average demand for high temperature (HT) and low temperature (LT) heating, for cooling and electricity in typical days of each month

It was found that heating demand displays significant seasonal variations: as can be observed in Figure 1, heating demand is maximum in April, when milk production is at its peak, and minimum in November, when only ripening of previously produced cheese is performed. This is also confirmed by the calculated profiles of cooling demand by storage cells (down to 5°C) and maturation cells (which are kept at constant temperature of 12 °C), by the measured electric load profiles and by the calculated net electricity demand (without cooling uses). The net electricity demand and the useful cooling load (expressed in thermal kW) are shown in Figure 2 for April and November.

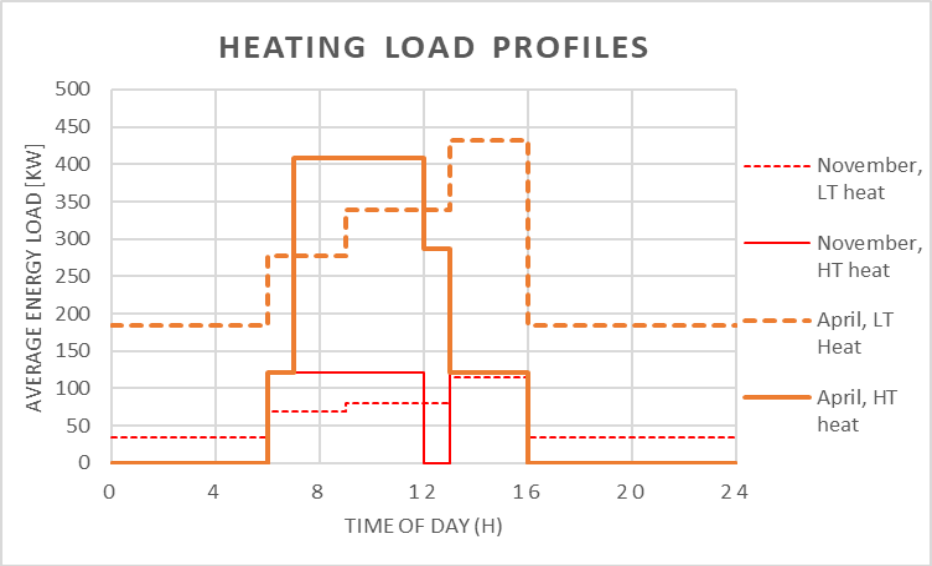

Figure 1. Heating load profiles of cheese factory on typical days in April and November

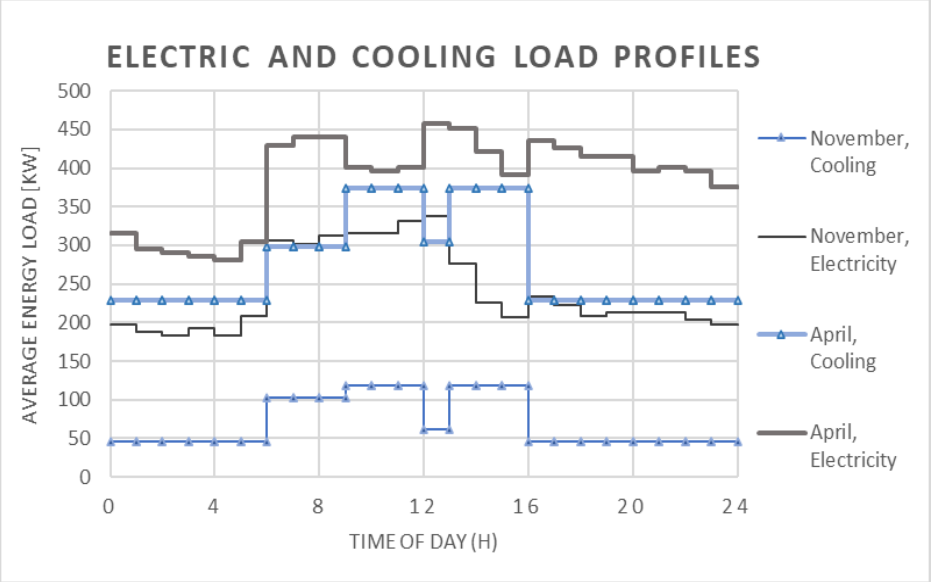

Figure 2. Cooling and electric load profiles of cheese factory on typical days in April and November

Overall, the energy demand of the dairy plant mainly depends on the quantities of milk processed, while is it minimally related to climate patterns. For this reason, the energy profiles of the plant were taken as reference of a generic multi-product cheese production plant in Italy, so that energy conditions more commonly available on the Italian mainland, e.g., as to natural gas as a fuel and as to electricity mix and prices, have been used for calculations.

On average the useful heating demand is about 0.28 kWh/kg of processed milk, which is in line with the values reported by [2] and [3], while the electricity demand is about 0.0135 kWh/kg, in line with the values reported in [12].

3 METHODOLOGY: OPTIMIZATION MODEL AND DATA

A mixed integer linear programming model was developed and implemented in GAMS [8]. The whole model structure, including energy balances, builds upon the models presented in [14][24][30][31].

3. 1 Solar collectors

The objective function to be minimized is the annual equivalent costs C_{total} , calculated according to equation 1 as the sum of operational expenses, which include the costs of natural gas, electricity, and maintenance as well as a carbon cost component depending on the carbon price CO_2pr and on carbon equivalent emissions associated with electricity and fuel consumption (via emissions factors *CO2em_el* and *CO2em_ng*, respectively), plus capital expenses for equipment, expressed in general terms as a linear function of nominal capacity *P* as in equation 1 and weighted by the capital recovery factor *crf* expressed in equation 2.

For each type of technology *t*, it is assumed that the nominal power of the equipment may assume all values between the minimum and the maximum commercially available capacity, denoted as *minCPt* and *maxCPt*, respectively (equation 3). Binary variables δ_t in equation 1 and 3 account for the size independent component of capital costs and equal 1 if and only if technology *t* is selected by the optimization procedure to enter the final configuration.

Moreover, for each time step (hour) *h* of month *m* the output flow of technology *t* cannot exceed the installed nominal power *P*, as guaranteed by equation 4.

$$Min\ C_{total} = \sum_t \sum_h \sum_m (c\_op_t F_{t,h,m} d_m + c\_el_{h,m} \frac{F_{t,h,m}}{\eta_t} d_m + c_{ng} \frac{F_{t,h,m}}{\eta_t H_i} d_m + CO_2pr \cdot (CO2_{ng} + CO2_{el}) + crf \cdot \sum_t [CAPf_t \delta_t + CAPv_t P_t] \quad (1)$$

$$crf = \frac{i(1+i)^n}{(1+i)^n - 1} \quad (2)$$

$$\delta_t \cdot MINCP_t \leq P_t \leq \delta_t \cdot MAXCP_t \quad (3)$$

$$0 \leq F_{t,h,m} \leq P_t \quad (4)$$

Additional energy balance equations are introduced for each energy conversion technology introduced in the model superstructure represented in figure 3.

In general terms, the output energy flows $F_{t,h,m}$ in each time step *(h,m)* are linked to input energy $I_{t,h,m}$ according to equations 5 by energy efficiencies, denoted in equations 1 and 5 with the generic symbol η.

$$I_{t,h,m} = \frac{F_{t,h,m}}{\eta_t} \quad (5)$$

The use of the symbol η for efficiency is straightforward when the input is fuel (natural gas) as in the case of CHP units or boilers, or for heat exchangers and pumping systems within the external waste heat transfer system, whereas it should be understood as an alias for EER in the case of refrigeration cycles.

The efficiencies of real CHP or pumping systems should be actually represented as efficiency curves depending on load factors. However, they are approximated as fixed efficiencies to make the optimization problem linear and tractable. In particular, for CHP units, minimum part load constraints are introduced by using binary variables as in [31], and efficiencies are assumed to be constant down to the minimum part load and with fixed power to heat ratios (the efficiency values assumed and corresponding literature references are summarized in table 2). Binary variables are also introduced as in [30][31] to model Italian tax exemption quotas for natural gas feeding CHP systems, which currently apply up to a threshold of 0.2085 Nm^3 of natural gas per electric kWh.

For the conversion technologies that are directly linked to end uses in figure 3, the energy balance constraints the total output to match the corresponding end use energy demand *Dem* in each time step.

For instance, the energy balance reported in equation 6 applies to cooling demand

$$F_{compcool,h,m} + F_{abscool,h,m} = D_{cooling,h,m} \quad (6)$$

The end uses include the types of energy flows required at the cheese factory as characterized in section 2, i.e. cooling energy, low temperature and high temperature process heat, and net electricity for equipment and lightning. In addition, excess heat dissipation is also modelled as an end use demand. The heat dissipation technology considered in this study is dry cooling, which is used to dissipate waste heat *WH* from the remote industrial waste heat source in case district heating is not implemented or when waste heat flows exceed the demand by the cheese factory, as well as waste heat from condensation in refrigeration cycles $WH_{cooling}$. The latter is calculated according to equation 7 (e.g. for vapour compression refrigeration cycles) as a function of the useful cooling output.

$$F_{compcool,h,m} \cdot \left(1 + \frac{1}{EER_{compcool}}\right) + F_{abscool,h,m} \cdot \left(1 + \frac{1}{EER_{abscool}}\right) = WH_{cooling,h,m} \quad (7)$$

3.1.1 Solar collectors

Compared with previous models reported in relevant literature, the reference energy system, which is diagrammed in Figure 3, is expanded to include solar collectors. The optimization procedure selects the best mix in terms of number (discrete, with fixed area of individual panels), type and inclination (30° or 45°) of solar collectors. The collector efficiency is modelled with the Hottel-Whillier-Bliss equation (8)

$$\frac{Q_u}{A_c} = F_R(\tau\alpha)E_h - F_R U_L\left(T_{fi} - T_{a,ext}\right) \quad (8)$$

The collector heat removal factors F_R by the effective transmittance-absorptance products (τα) and overall heat loss coefficient U_L have been derived from the commercial database Retscreen [32] for Viessmann flat and evacuated collectors and they are reported in Table 2. External temperatures have been determined according to the UNI 10349 standard, while hourly radiation has been determined for a reference location on the Italian mainland (45° latitude) using the utilizability function method with the Clark algorithm [33].

3.1.2 Thermal storage

Two separate hot water tanks, coupled to the solar collector and boilers (steady state temperature 70°C), and to the cogeneration system and boilers (steady state temperature 90°C), can be selected and sized by the optimization procedure as continuous variables**.**

The heat balance equation 9 for heat accumulators requires that, in each time step *h* of the reference day for month *m* and for each accumulator, the stor level $SL_{h,m}$ equals the storage level at the previous time step $SL_{h-1,m}$ plus the additional charging flows $Fstch_{t,h,m}$ from all the heat generation units feeding each tank as described minus the sum of discharge flows $Fstdis_{t,h,m}$ to each heat user supplied by the tank.

$$SL_{h,m} = SL_{h-1,m} + \sum_{t \in heatgen} Fstch_{t,h,m} + \sum_{t \in heatus} Fstdis_{t,h,m} \tag{9}$$

The model is approximated in that heat losses are assumed to be negligible and the charging and discharging efficiencies are assumed to be unitary.

3.1.3 District heating model

For the district heating network, the annual equivalent system costs, which have been written in a general form for generic equipment in equation 1, include the annualized capital costs of network construction, including pipe and excavation costs, pumping systems and heat exchangers, plus the operational costs of network maintenance and electricity demand for pumping, as shown in equation 10.

$$C_{DH} = c_{manDH} \cdot CAPf_{\Phi}\delta_{\Phi} + \sum_{h,m,\Phi} DHF_{h,m,\Phi} \cdot pumpf_{\Phi} \cdot d_{h,m} \cdot c_{el\,h,m} + crf \cdot \left[CAPf_{pump}\,\delta_{pump} + CAPv_{pump}\,P_{pump} + 2 \cdot CAPf_{heatx}\,\delta_{heatx} + 2 \cdot CAPv_{heatx}\,P_{heatx} + \sum_{d}(CAPDHf_{\Phi}\delta_{\Phi} \cdot LDH)\right] \tag{10}$$

The electric energy required for pumping is a function of the heat flow *DHF* entering the pipes in each time step by a pumping energy factor *pumpf*, which is calculated for each diameter class with a linearization approach based on interpolation as proposed in [24].

It can be observed that the capacities of pumps and of the two heat exchangers are modelled as continuous variables plus the binary component δ, whereas pipes come in discrete sizes (diameter class Φ). Pipe selection is thus modelled exclusively by the binary variable δ_{Φ}, which equals 1 if a pipe of diameter class Φ is selected. Equation 11 constrains the optimization procedure to select at most one diameter class, while

equation 12 shows how heat losses along district heating pipes are accounted for by the linear heat loss factor hlf_Φ. hlf_Φ is expressed in kW/m and is calculated for each diameter class Φ with equation 13, where U_Φ is the thermal transmittance of pipes in kW/m K for each diameter class, and T_f , T_r, and T_s are the average flow, return, and soil temperature, respectively.

$$\sum_{\Phi} \delta_{\Phi} \leq 1 \tag{11}$$

$$DHFout_{h,m,\Phi} = \left(DHFin_{h,m,\Phi} - hlf_{\Phi} \cdot LDH\right) \tag{12}$$

$$hlf_{\Phi} = U_{\Phi}\left[\left(T_f + T_r\right) - 2T_s\right] \tag{13}$$

3.1.4 Environmental constraints

Environmental constraints are applied by calculating the carbon equivalent emissions (GWP100) during the equipment lifetime. To evaluate total emissions, the contribution of construction materials is also evaluated as shown in equation 14,

$$CO2_{total} = \sum_h \sum_m \left[\sum_{t \in Tel} CO2em_{el} \frac{F_{t,h,m}}{\eta_t} d_m + \sum_{t \in Tfuel} CO2em\_ng \frac{F_{t,h,m}}{\eta_t H_i} d_m + \sum_{t \in T} CO2em\_M \frac{P_t}{n}\right] \tag{14}$$

and added to the direct emissions from fuels (2.6 kg/Nm^3 of natural gas, having a calorific value of 9.6 kWh/Nm^3) and to the indirect emissions associated with the average national electricity generation mix, obtained from ISPRA [22], which equals 0.323 tCO_2eq/kWh. However, carbon price is only applied to energy related components as shown in the objective function (1).

3.2 Technical and economic data for model implementation

The technical and economic data used for implementing the model described in the previous section and graphically represented by the reference energy system of figure 3 are summarized in tables 2 and 3 for energy conversion equipment and district heating pipes, respectively.

As shown in figure 3, both reciprocating internal combustion engines and micro gas turbines are considered as technology options for cogeneration. Because of the limited size range of commercially available microturbines, their capacity is modelled with binary variables to assume a limited range of discrete values (30, 60, 100, 200 or 250 kWel, respectively), unlike the capacity of reciprocating engines, which, like all equipment apart from district heating pipes, is modelled as a continuous variable that can assume any value, in this case ranging between 200 and 1000 kWel.

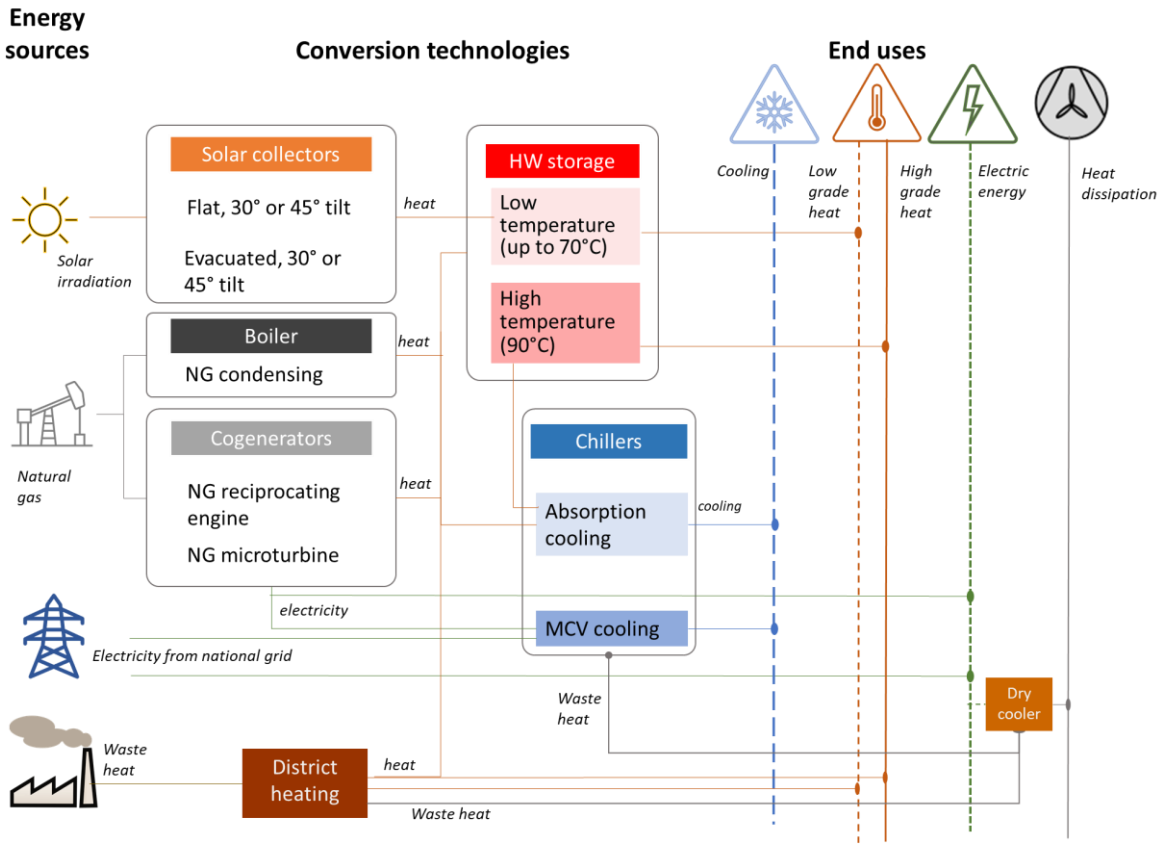

Figure 3. Scheme of the reference energy system

Table 2. Technical data and carbon footprints of energy conversion equipment

Technology	**Size reference unit (sru)**	**Efficiency and operation related parameters**	**Materials related carbon footprint *CO2em_M* [kgCO2eq/sru]**	**Size independent capital cost component $CAPf_t$ [€]**	**Size dependent capital cost component $CAPv_t$ [€/ sru]**	**References**
NG Condensation boiler	kW	η=96% for LT uses, 85% for HT uses	28.26	5072	54	[10][11]
NG Reciprocating engine	kWel	η_{el}=37%, down to 20% minimum part load.P/H ratio = 86%	218.8	122959	973	[12] [13] [14]
NG Microturbine	kWel	η_{el}=30%, down to minimum 50% part load. P/H ratio = 66%	58.73	61716	2067	[12] [13] [14] [15], [16]

Absorption Chiller	kW	EER= 0,7	26.01	95000	94	[10] [17]
MVC Chiller	kW	EER= 4	4	20000	112	[10] [17]
Flat solar thermal panel	m^2	Fr(τα)=0,723 Fr(U_L)=4,159 W/m^2 °C	88	1995	305	[16] [18][19]
Evacuated solar thermal panel	m^2	Fr(τα)=0,592 Fr(U_L)=1,724 W/m^2 °C	78.58	3515	538	[16] [18][19]
Thermal storage (hot water)	m^3	Heat losses treated as negligible	602	0	938	[4] [16][18][19]
District heating pump	kWe					
Heat exchangers	kW					

Table 3. Technical data and carbon footprints of district heating system components

The capital costs and the construction carbon footprint of dry coolers are not considered since it is assumed that, as to refrigeration systems, their costs and footprint already include condensation equipment, whereas, as to the dissipation of industrial waste heat, it is assumed on the side of caution that the capacity of existing equipment remains unchanged even if the need for dissipation is reduced or eliminated by injecting excess heat in the district heating system. In that case, only the operation of dissipation systems is assumed to change, which leads to a reduction of related electricity demand, asssumed to be proportional to the waste heat dissipation demand according to equation 15

$$Fel_{h,m} = \sum_t \kappa \cdot WH_{t,h,m} \qquad (15)$$

Where κ = 0.03 based on previous studies on manufacturers catalogues [22][42].

For all equipment a lifetime n of 15 years, and an interest rate i = 12% is considered to calculate the capital recovery factor.

Table 3 shows the district heat pipe diameters considered, the corresponding capital costs and heat loss coefficients, which are evaluated based on the data reported in [22], assuming a flow temperature of 90°C, a return temperature of 70°C, and an average soil temperature of 15°C. The associated minimum and

maximum heat flows are also calculated for these temperature ranges, assuming that regulation is performed with a fixed temperature difference and by varying water flows and velocities between 0,5 m/s and 3 m/s, and that a further fine regulation of temperature is possible by augmenting return temperature up to 80°C when velocity reaches the lower edge of the acceptable range. These values of velocities are also used to calculate the annual pumping electricity demand factors $pumpf_{\phi}$ reported in Table 3 as in [24] by linear regression (with intercepts set to zero) of friction loss calculated with standard Hazen-Williams equations, which is then multiplied by mass flow rate and divided by the total efficiency of the pump to estimate absorbed power. Unlike in [24], the regression of the power demand as dependent variable is performed on transported heat flows as independent variables, rather than on volumetric flow rates, so that the $pumpf_{\phi}$ is straightforwardly expressed in kWe/kWth. The carbon emission coefficients *CO2em_M* associated with materials for pipe construction, including excavation, are obtained by interpolation based on the values reported in [22].

Maintenance costs are considered for boilers, cogeneration equipment, and district heating systems, whereas they are assumed to be negligible or invariant for the remaining components. Maintenance cost factors are assumed to equal 0.001 € per kWh of generated thermal energy for boilers, 0.022 € per kWhe of generated electricity for internal combustion engines, 0.011 € per kWh of generated electricity for microturbines, and to equal yearly 2% of the total capital costs for district heating [30].

Natural gas and electricity tariffs have been derived at the time of the analysis (September 2021) from the national ARERA website [21] for industrial customers in the proper energy consumption class. In particular, a single tier tariff of 0.416 €/Nm^3 applies to natural gas feeding boilers, whereas the tax exemption quota of 0.01 €/Nm^3 applies to natural gas up to the previously mentioned threshold of specifc consumption. For electricity, time-of-use based tariffs apply, equalling 177.13 €/MWh in peak hours (8-18), 139.56 €/MWh in off-peak hours (23-7) and 174.44 €/MWh in the remaining time steps.

4 RESULTS AND DISCUSSION

The mixed integer linear programming model implementation resulted in a total of about 58200 variables and 38700 constraints. The optimization was solved with the solver CPLEX 12.7.1 [45].

To explore the role of industrial waste heat as a low carbon energy source, a virtual remote industrial waste heat source has been devised, and six scenarios are defined depending on the level of the available waste heat flow and on the distance between source and user. It is assumed that the industrial waste heat flow is steadily available 24/7, and that its value equals either the average total heating flow reported in table 1, ½ of that flow or 2 as much. These scenarios are denoted in table 4 as *WH=AVG*, *WH=1/2 AVG*, and *WH=2 AVG* configurations, and they correspond to waste heat flows of 126.1 kWt, 252.2 kWt, and 504.4 kWt. For each

WH flow level, source-user distances (i.e. length of district heating, *LDH*) of 300 m and of 1000 m, respectively, are selected for investigation based on feasibility limits reported in [22]. For each source-user distance and waste heat flow level scenario, minimum cost solutions are determined for two carbon price levels, i.e. *CO2price*=0 and *CO2price*=50 €/tCO_{2eq}, respectively. Moreover, a baseline scenario is also defined for each *WH* flow level, where only traditional technologies, i.e. natural gas condensation boilers, electricity supply from the grid, and cooling and refrigeration with mechanical vapour compression chillers. This yields a total of fifteen scenarios summarized in table 4, which reports the optimized capacity for all pieces of equipment in each scenario.

4.1 Results for reference conditions

Table 4 shows that a natural gas boiler of 748 kW and a vapor compression cooling system of 384 kW of useful thermal energy are able to meet energy demand by the cheese factory in the baseline scenario. In optimized scenarios, industrial waste heat recovery via district heating belongs to least cost configurations only in *WH=AVG* and *WH=2 AVG* scenarios, and only with a distance between source and user of 300 m. If less heat is available or if it is available at a distance of 1000 m, cogeneration is the preferred option, and an absorption cooling capacity of less than 200 kW of cooling energy is installed to exploit waste heat from cogeneration to meet base cooling loads. Table 5 further clarifies that cogenerators are installed in all the optimized configurations, and that heat storage at high temperature is coupled with CHP to enable the system to meet the electricity demand of the industry, minimizing the amounts of purchased electricity.

Absorption cooling meets between 47.1% and 66.3% of the total cooling energy demand, with higher shares if district heating is activated.

When waste heat is shared via district heating, it is mainly used to meet the factory high temperature demand, with shares up to 72.9% of the total demand, while low temperature demand is covered by heat recovery from cogenerators. The cogenerator capacity is always in the order of 500 kW_e, and it is decreased by about 10-15% when district heating is introduced. CHP units are always single internal combustion engines. Microturbines are never included within optimal CHP configurations because their smaller size, higher specific capital costs, and lower efficiencies are not compensated by lower maintenance costs.

Comparing table 4 and 5, we can observe that larger thermal storage is installed when district heating is introduced, in order to take advantage of large flows of heat available when the user's demand is low. Since operational costs for district heating are much lower than natural gas costs, is the source is close enough it pays off to install a large storage even if its use is relatively unfrequent. In table 5, in fact, we see that only about 5% of high temperature heat demand comes from storage in scenarios with district heating, against about 30% when CHP systems alone are installed. In that case, storage capacity is smaller but its use is much more intensive. If district heating is selected, the size of pipes, pumps and heat exchangers is always determined by the available waste heat flow, rather than by demand levels.

Table 4 Optimized capacities of equipment and district heating by scenario

		WH = ½ AVG Total heating demand						WH = AVG Total heating demand						WH = 2 · AVG Total heating demand					
		CHP [kWe]	**DH [kWth]**	**NG Boiler [kWth]**	**Cooling [kWth]**	**Solar panel [m²]**	**Thermal Storage [m³]**	**CHP [kWe]**	**DH [kWth]**	**NG Boiler [kWth]**	**Cooling [kWth]**	**Solar panel [m²]**	**Thermal Storage [m³]**	**CHP [kWe]**	**DH [kWth]**	**NG Boiler [kWth]**	**Cooling [kWth]**	**Solar panel [m²]**	**Thermal Storage [m³]**
BASE	***No CHP, No DH, No Solar***	0	0	748	384 Comp	0	0	0	0	748	384 Comp	0	0	0	0	748	384 Comp	0	0
CO2price 0 €/t	***LDH=300 m***	497	0	0	199 Abs 374 Comp	0	29.75	467	252.25	0	230 Abs 175 Comp	0	54.75	468	504	0	231 Abs 174 Comp	0	54.75
	LDH=1000 m	497	0	0	199 Abs 374 Comp	0	29.75	501	0	0	199 Abs 374 Comp	0	28.75	504	0	0	199 Abs 367 Comp	0	29.5
CO2price 50 €/t	***LDH=300 m***	476	0	0	185 Abs 374 Comp	0	36	442	252.25	0	214 Abs 169 Comp	0	73.5	426	504	0	202 Abs 181 Comp	0	71.5
	LDH=1000 m	476	0	0	185 Abs 374 Comp	0	36	477	0	0	189 Abs 374 Comp	0	35.5	484	0	0	193 Abs 374 Comp	0	33.5

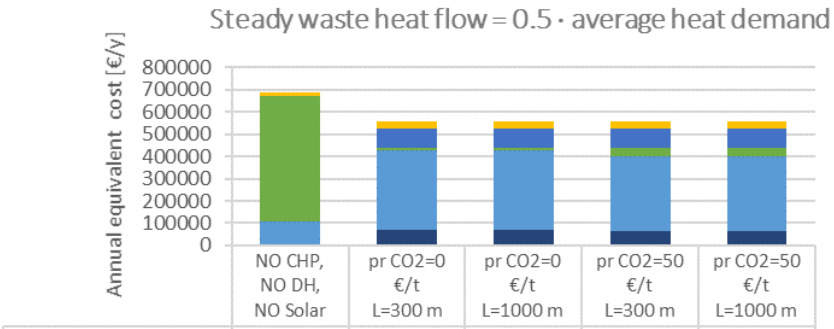

	NO CHP, NO DH, NO Solar	pr CO2=0 €/t L=300 m	pr CO2=0 €/t L=1000 m	pr CO2=50 €/t L=300 m	pr CO2=50 €/t L=1000 m
Other equipment CAPEX	15909	30497	30497	31300	31300
SOLAR CAPEX eq	0	0	0	0	0
DH CAPEX eq	0	0	0	0	0
CHP CAPEX eq	0	89127	89127	86030	86030
Electricity OPEX	566083	11815	11815	38051	38051
Natural gas OPEX	103669	356102	356102	336558	336558
O&M	2014	69568	69568	65750	65750

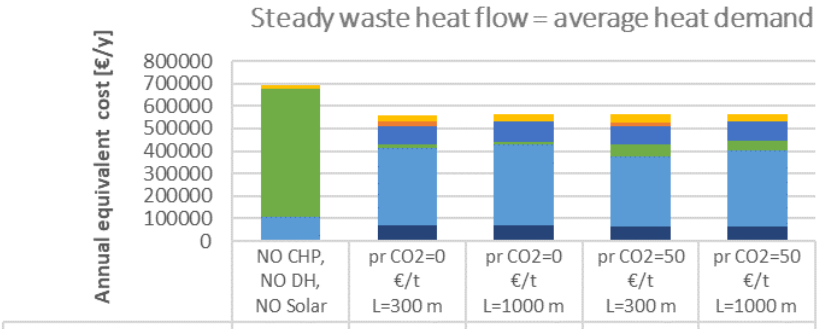

	NO CHP, NO DH, NO Solar	pr CO2=0 €/t L=300 m	pr CO2=0 €/t L=1000 m	pr CO2=50 €/t L=300 m	pr CO2=50 €/t L=1000 m
Other equipment CAPEX	15909	31599	30338	34257	31266
SOLAR CAPEX eq	0	0	0	0	0
DH CAPEX eq	0	16601	0	16601	0
CHP CAPEX eq	0	84828	89622	81261	86278
Electricity OPEX	571520	11724	11955	51670	39524
Natural gas OPEX	103669	346249	359478	314764	338942
O&M	2014	69905	70227	63754	66216

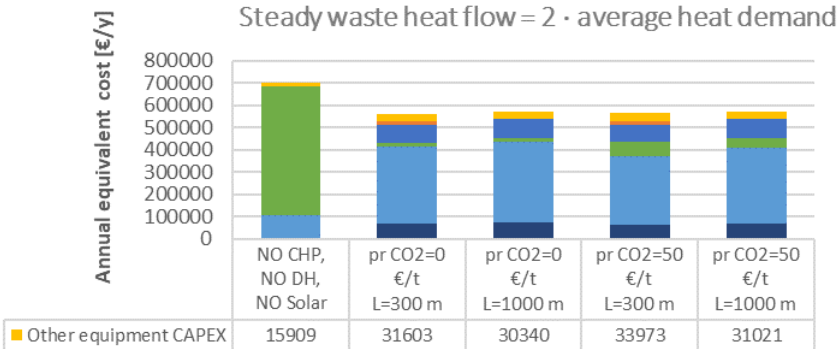

	NO CHP, NO DH, NO Solar	pr CO2=0 €/t L=300 m	pr CO2=0 €/t L=1000 m	pr CO2=50 €/t L=300 m	pr CO2=50 €/t L=1000 m
Other equipment CAPEX	15909	31603	30340	33973	31021
SOLAR CAPEX eq	0	0	0	0	0
DH CAPEX eq	0	17120	0	17120	0
CHP CAPEX eq	0	84915	90131	78916	87269
Electricity OPEX	582392	11555	13063	61915	41334
Natural gas OPEX	103669	346903	365735	309627	344330
O&M	2014	70103	71450	62821	67268

Figure 4. Breakdown of annual equivalent systems costs by scenario

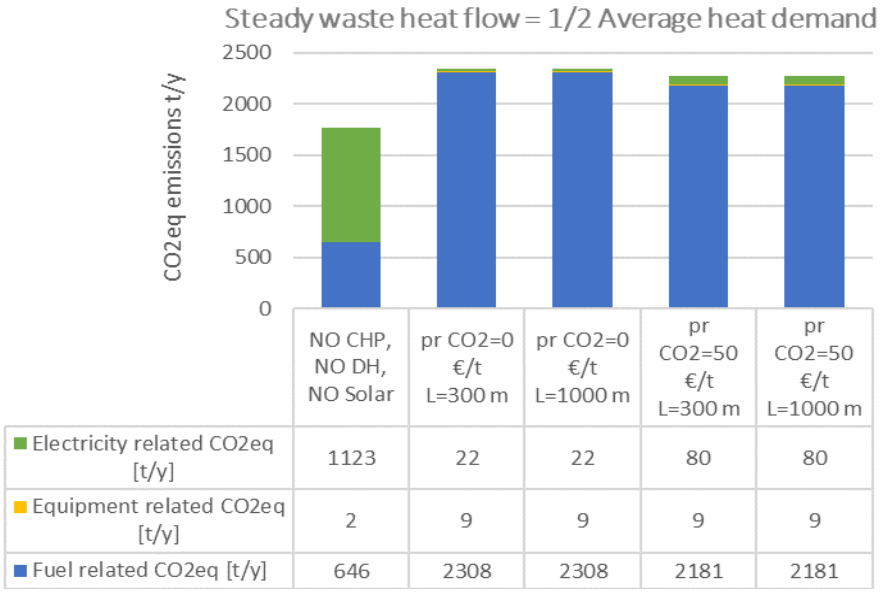

	NO CHP, NO DH, NO Solar	pr CO2=0 €/t L=300 m	pr CO2=0 €/t L=1000 m	pr CO2=50 €/t L=300 m	pr CO2=50 €/t L=1000 m
Electricity related CO2eq [t/y]	1123	22	22	80	80
Equipment related CO2eq [t/y]	2	9	9	9	9
Fuel related CO2eq [t/y]	646	2308	2308	2181	2181

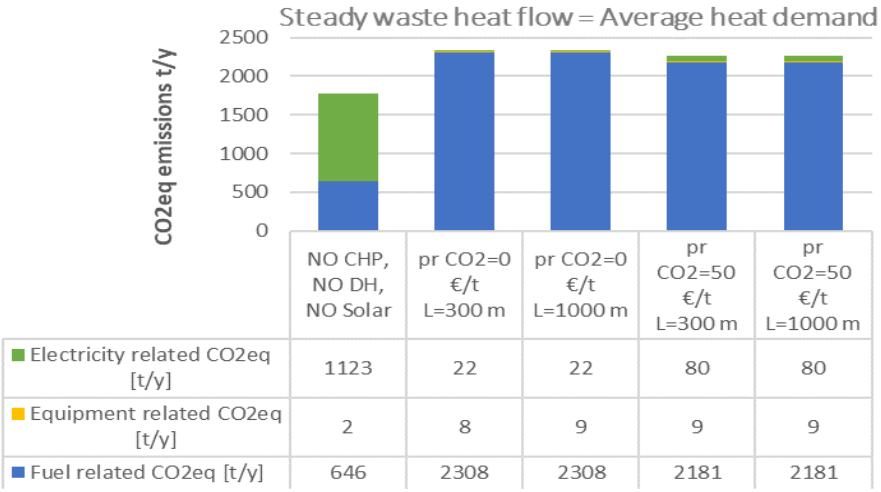

	NO CHP, NO DH, NO Solar	pr CO2=0 €/t L=300 m	pr CO2=0 €/t L=1000 m	pr CO2=50 €/t L=300 m	pr CO2=50 €/t L=1000 m
Electricity related CO2eq [t/y]	1123	22	22	80	80
Equipment related CO2eq [t/y]	2	8	9	9	9
Fuel related CO2eq [t/y]	646	2308	2308	2181	2181

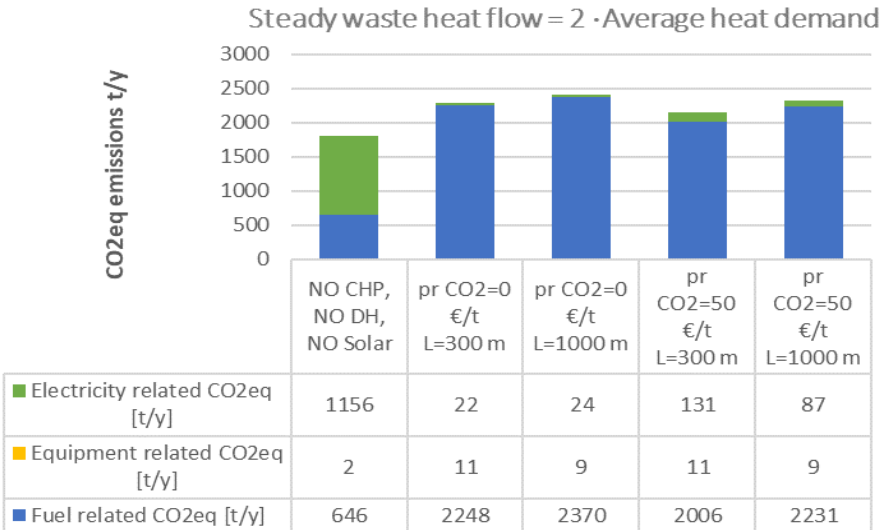

	NO CHP, NO DH, NO Solar	pr CO2=0 €/t L=300 m	pr CO2=0 €/t L=1000 m	pr CO2=50 €/t L=300 m	pr CO2=50 €/t L=1000 m
Electricity related CO2eq [t/y]	1156	22	24	131	87
Equipment related CO2eq [t/y]	2	11	9	11	9
Fuel related CO2eq [t/y]	646	2248	2370	2006	2231

Figure 5. Breakdown of annual carbon equivalent emissions by scenario

Table 5 Coverage of high temperature (HT) and low temperature (LT) heating demand, of electricity demand, and of cooling demand by different technologies and scenarios

		CO2 =0 €/t		CO2 =50 €/t	
	DH Length [m]	*300*	*1000*	*300*	*1000*
1/2 Avg Dem	% CHP Heat on HT	73.8%	73.8%	65.9%	65.9%
	% DH heat on HT	0.0%	0.0%	0.0%	0.0%
	% Stored heat on HT	26.2%	26.2%	34.1%	34.1%
	% Boiler on HT	0.0%	0.0%	0.0%	0.0%
	% CHP Heat on LT	100.0%	100.0%	100.0%	100.0%
	% DH heat on LT	0.0%	0.0%	0.0%	0.0%
	% Stored heat on LT	0.0%	0.0%	0.0%	0.0%
	% Boiler on LT	0.0%	0.0%	0.0%	0.0%
	% Solar on LT	0.0%	0.0%	0.0%	0.0%
	% Purchased Electricity on total	2.1%	2.1%	7.5%	7.5%
	% Absorption cooling energy on total	49.0%	49.0%	47.1%	47.1%
Avg Dem	% CHP Heat on HT	26.9%	70.5%	24.1%	68.0%
	% DH heat on HT	67.6%	0.0%	71.2%	0.0%
	% Stored heat on HT	5.5%	29.5%	4.7%	32.0%
	% Boiler on HT	0.0%	0.0%	0.0%	0.0%
	% CHP Heat on LT	99.8%	100.0%	90.7%	100.0%
	% DH heat on LT	0.2%	0.0%	9.3%	0.0%
	% Stored heat on LT	0.0%	0.0%	0.0%	0.0%
	% Boiler on LT	0.0%	0.0%	0.0%	0.0%
	% Solar on LT	0.0%	0.0%	0.0%	0.0%
	% Purchased Electricity on total	2.1%	2.1%	10.7%	7.7%
	% Absorption cooling energy on total	65.2%	49.7%	66.3%	47.9%
2Avg Dem	% CHP Heat on HT	26.6%	72.5%	23.8%	67.2%
	% DH heat on HT	68.7%	0.0%	72.9%	0.0%
	% Stored heat on HT	4.7%	27.5%	3.3%	32.8%
	% Boiler on HT	0.0%	0.0%	0.0%	0.0%
	% CHP Heat on LT	99.8%	100.0%	91.5%	100.0%
	% DH heat on LT	0.2%	0.0%	8.5%	0.0%
	% Stored heat on LT	0.0%	0.0%	0.0%	0.0%
	% Boiler on LT	0.0%	0.0%	0.0%	0.0%
	% Solar on LT	0.0%	0.0%	0.0%	0.0%
	% Purchased Electricity on total	2.1%	2.2%	12.6%	8.0%
	% Absorption cooling energy on total	65.7%	51.2%	64.3%	49.6%

Figure 4 shows that both CHP alone (in the 1000 m *LDH* scenarios) as well as the combination of CHP and district heating preferred in the 300 m *LDH* scenarios lead to similar savings, in the order of 19%, compared with the baseline scenario. The cost advantage of solutions including district heating with 300 m *LDH* is only slightly higher if more heat is available and it is mainly due to fuel savings.

Interestingly, natural gas boilers and solar panels are never installed, even for carbon prices of 50 €/t. Furthermore, a carbon price of 50 €/t is also not sufficient to make heat supply from a source at 1000 m from the user economically preferable to independent cogeneration at the dairy industry site. In other words, a 50 €/t carbon price does not substantially affect the structure of economically optimal configurations and, as shown in figure 5, it only determines a slight reduction in total carbon emissions, in the order of 3-5%. Figure 5 highlights that this reduction is mainly linked to a reduced use of natural gas, which is achieved:

- by installing smaller engines and absorption chillers, and increasing electricity purchase, especially for cooling, if waste heat recovery through district heating is not viable (all ½ AVG scenarios and 1000 m LDH scenarios);
- By increasing heat supply from district heating with enhanced heat storage capacities when district heating is feasible. Also in that case, smaller cogenerators and smaller absorption cooling systems are installed than in null carbon price scenarios.

It should be stressed that, as shown in figure 5, minimum cost scenarios, regularly involving cogeneration, always lead to increased carbon emissions compared with the baseline scenario. This is due to the low emission factor for electricity, in turn depending on the high share of renewable sources in the national electricity mix.

4.2 Sensitivity to emission reduction constraints

From the discussion above we deduce that cogeneration is economically attractive but leads to higher emissions than traditional technologies. This is further confirmed by performing a parametric analysis for the *WH=AVG, LDH=300 m* scenario and for the *WH=AVG, LDH=1000 m* scenario, by setting and progressively reducing upper bounds to energy related annual carbon equivalent emissions. Starting from the minimum cost solution, carbon equivalent emissions are reduced by 15%, 30%, 45% percent (that is from 2265 t/y to 1246 t/y) up to the maximum feasible emission reduction percentage, which equals 48% (corresponding to CO_2eq emissions of 1231 t/y).

The results of this analysis are reported in Figure 6, as to the total and average costs, as well as in table 6, which shows how technical configurations change when more restrictive limits to carbon emissions from the whole energy supply system are imposed. It can be observed that specific costs of emission reduction are much lower when *LDH=300 m* scenario.

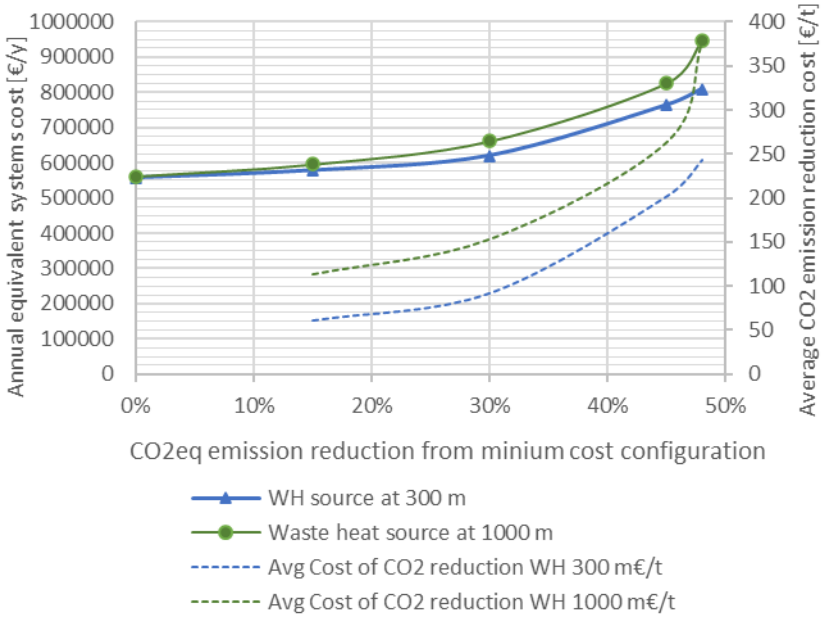

Figure 6. Total and average specific costs of optimized solutions under emission reduction constraints

Table 6 Optimized capacities of main equipment under emission reduction constraints

		CO2eq emission reduction from minimum cost				
		0%	15%	30%	45%	48%
Main technical features, WH source at 300 m	CHP capacity [kW_e]	467	372	250	0	0
	DH capacity [kWt]	252	252	252	252	252
	Hot Storage volume [m^3]	54.75	122.00	59.25	122.25	122.00
	Total solar panel surface [m^2]	0	0	0	1105	1485
Main technical features, WH source at 1000 m	CHP capacity [kW_e]	501	336	254	0	0
	DH capacity [kWt]	0	0	252	252	252
	Hot Storage volume [m^3]	28.75	140.10	121.25	120.25	119.75
	Total solar panel surface [m^2]	0	0	0	1303	1888

When more restricted bounds to carbon emission are imposed, waste heat recovery through district heating is introduced, in combination with smaller CHP engines and, as shown in table 7, with mechanical vapour compression cooling alone. Recovering waste heat from a relatively small but steady heat source at 1000 m distance from the user is preferred to installing solar panels, which are only introduced when emission reduction percentages of 45% are imposed. In that case, engines are not installed and flat solar panels with a 45° tilt are selected.

As shown in table 7, district heating, in combination with peak load boilers, is mainly used to meet high temperature heat demand, while solar panels allow to meet 45% to 48% of the yearly low temperature heat demand of the cheese factory. Average costs of emission reduction at this point are in the order of 260 €/tCO_{2eq}, while they reach about 200 €/tCO2eq if the waste heat source is located at 300 m.

Table 7 Energy demand coverage under emission reduction constraints

		CO2eq emission reduction				
		0%	15%	30%	45%	48%
HT heat	%DH	67%	71%	54%	85%	85%
	%CHP Heat	27%	24%	18%	0%	0%
	%NG BOILER	0%	0%	0%	15%	15%
	%HT STORAGE	6%	5%	28%	0%	0%
LT Heat	%DH	0%	33%	30%	17%	9%
	%CHP Heat	100%	67%	70%	0%	0%
	%Solar	0%	0%	0%	45%	48%
	%NG BOILER	0%	0%	0%	23%	20%
	%LT STORAGE	0%	0%	0%	15%	23%
Cooling	%ABS cool	65%	54%	0%	0%	0%
Electricity	%Electric purchase	2%	31%	65%	100%	100%

4.3 Sensitivity to changes in energy prices

Recent dramatic changes in energy prices confirmed the importance of exploring the sensitivity of design choices to market conditions.

In this work, natural gas and electricity prices have been varied by the coefficients reported in figure 7, where 1 represents the reference conditions assumed above. Independent variations of gas and electricity prices from -50% (0,5) to +100% (2) have been investigated for the *WH=AVG, LDH=300 m* scenario. Based on the analysis presented in sections 4.1 and 4.2, the shares of district heat on high temperature heat demand, of absorption cooling on total cooling demand, and of purchased electricity on total electricity demand have been taken as proxies for describing the systems configuration and behaviour.

Figure 7 shows that for low electricity prices and high gas prices (triangular lower matrix) district heating is installed and its contribution to heat demand coverage is enhanced up to 84.8%, as cogeneration is economically unfeasible or suboptimal. Absorption cooling is only performed in combination with cogeneration, although absorption chillers could theoretically run on district heat (see figure 3). That is the case of triangular upper matrixes in figure 7, which correspond to low costs of natural gas: in that case, trigeneration with CHP engines is the preferred solution.

NG price↓ El price→	0.5	0.75	1	1.5	2
0.5	0.0%	0.0%	0.0%	0.0%	0.0%
0.75	84.6%	0.0%	0.0%	0.0%	0.0%
1	84.8%	84.8%	67.6%	70.0%	70.0%
1.5	84.8%	84.8%	82.8%	68.6%	69.0%
2	84.8%	84.8%	84.8%	72.2%	66.9%

Share of DH on HT heat demand

NG price↓ El price→	0.5	0.75	1	1.5	2
0.5	0.0%	49.0%	52.2%	58.9%	56.8%
0.75	0.0%	47.0%	51.0%	52.0%	52.3%
1	0.0%	0.0%	65.2%	67.8%	68.1%
1.5	0.0%	0.0%	0.0%	74.1%	72.8%
2	0.0%	0.0%	0.0%	64.1%	79.1%

Share of absorption cooling energy on total cooling demand

NG price↓ El price→	0.5	0.75	1	1.5	2
0.5	100.0%	1.8%	0.8%	0.0%	0.0%
0.75	100.0%	8.4%	1.2%	0.5%	0.0%
1	100.0%	100.0%	2.1%	0.5%	0.2%
1.5	100.0%	100.0%	76.6%	1.1%	0.2%
2	100.0%	100.0%	100.0%	20.8%	0.7%

Share of purchased electricity on total electricity demand

Figure 7. Sensitivity of demand coverage in optimized configurations to changes in natural gas (NG) and electricity (El) price

Along the diagonal and when both gas and electricity prices increase, district heat and cogeneration usually coexist. Thus, if a small but steady amount of waste heat is available within a 300 m radius, a combination of trigeneration and use of external waste heat is the least cost option to face high natural gas and electricity prices.

5 CONCLUSIONS

This study presented the synthesis and optimization of a hybrid polygeneration system designed to meet the energy demands of an Italian cheesemaking industry, which includes heating at various temperature levels, cooling, and electricity. An energy audit was performed to obtain hourly demand profiles for typical days in each month for a reference plant, which processes yearly more than eight million litres of milk.

The results confirm the evidence, emerging from previous studies and from the practice, that cheesemaking industries are ideal settings for trigeneration: in fact, the combination of internal combustion engines and optimally sized absorption cooling systems has been found to be the minimum cost solution for the analyzed

case study, leading to savings in annual equivalent systems costs in the order of 18-20% at reference conditions compared with baseline configurations (i.e. natural gas boilers, electricity supply from the grid and mechanical vapour compression cooling system). However, it is important to observe that fossil fuel based trigeneration, although energy efficient and economically attractive at reference conditions, may worsen carbon emissions performance at current electricity related emission factors, leading to a percentage increase of carbon emissions in the order of 30% of baseline configuration values. If carbon prices are included among annual equivalent costs, increments are only slightly smaller. If a zero-carbon waste heat source meeting at least the average heating demand by the milk processing plant is available within a radius of 300 m, district heating may be a viable option for external recovery and the dairy industry would be an ideal customer, despite its seasonal variation in operations and energy demand. Although the financial viability of cogeneration and trigeneration mainly relies on a steady heating demand, it has been found that external low carbon heat supply and cogeneration can be well combined, particularly to meet restrictions on carbon equivalent emission in a cost-effective way. In fact, industrial waste heat supply is also competitive with solar energy, which is only selected by the optimization procedure when emission limits become very stringent (45% emission reduction). The sensitivity analysis has also shown that for most combinations of electricity and natural gas prices, a combination of trigeneration and waste heat recovery from a zero emission source through district heating remains the least cost option, and district heating is alternative and not complementary to the installation of cogeneration systems only in the case of a simultaneous increase in natural gas prices and reduction in electricity prices, which was hardly observed on the Italian market up to these days. Future research in this context should be directed to incorporating additional renewable sources among the available technology options, and to devising optimization models and design procedures so that they are capable of identifying solutions with good environmental performance which are inherently robust to uncertain market conditions.

6 CREDIT AUTHORSHIP CONTRIBUTION STATEMENT

Damiana Chinese: Conceptualization, Data curation, Software, Investigation, Methodology, Formal Analysis, Writing – original draft. Pier Francesco Orrù: Data curation, Visualization, Investigation, Formal Analysis, Validation. Writing – review & editing. Giovanni Cortella: Methodology, Formal Analysis, Data curation, Writing – review & editing. Antonella Meneghetti: Methodology, Formal Analysis, Data curation, Writing – review & editing. Lorena Romeo: Conceptualization, Supervision, Project administration, Writing – review & editing. Miriam Benedetti: Conceptualization, Supervision, Project administration, Funding Acquisition, Writing – review & editing.

ACKNOWLEDGEMENTS

Part of this work was funded by the Program “Electrical System Research 2019–2021”, implemented under Program Agreements between the Italian Ministry for Economic Development and ENEA, CNR, and RSE S.p.A, Project 1.6 “Energy efficiency of industrial products and processes”, WP3.”

REFERENCES

[1] Notarnicola, B., Tassielli, G., Renzulli, P.A., Castellani, V., Sala, S. Environmental impacts of food consumption in Europe, *Journal of Cleaner Production*, 140, pp. 753-765，2017

[2] Canellada F., Laca A., Laca A., Díaz M., Environmental impact of cheese production: A case study of a small-scale factory in southern Europe and global overview of carbon footprint, *Science of The Total Environment*, Volume 635, 2018, pp. 167-177

[3] A Vagnoni, E., Franca, A., Porqueddu, C., Duce, P. Environmental profile of Sardinian sheep milk cheese supply chain: A comparison between two contrasting dairy systems, *Journal of Cleaner Production*, 165, pp. 1078-1089, 2017

[4] Palmieri N., Bonaventura Forleo M., Salimei E., Environmental impacts of a dairy cheese chain including whey feeding: An Italian case study, *Journal of Cleaner Production*, Volume 140, Part 2, 2017, pp. 881-889

[5] Piya Gosalvitr, Rosa Cuellar-Franca, Robin Smith, Adisa Azapagic, Energy demand and carbon footprint of cheddar cheese with energy recovery from cheese whey, *Energy Procedia*, Volume 161, 2019, pp. 10-16

[6] Quijera, J.A., Alriols, M.G., Labidi, J., Integration of a solar thermal system in a dairy process, *Renewable Energy*, 36 (6), pp. 1843-1853, 2011

[7] Allouhi, A., Agrouaz, Y., Benzakour Amine, M., Rehman, S., Buker, M.S., Kousksou, T., Jamil, A., Benbassou, A. Design optimization of a multi-temperature solar thermal heating system for an industrial process, *Applied Energy*, 206, pp. 382-392, 2017

[8] Hitesh Panchal, Romil Patel, Sudhir Chaudhary, D.K. Patel, Ravishankar Sathyamurthy, T. Arunkumar, Solar energy utilisation for milk pasteurisation: A comprehensive review, *Renewable and Sustainable Energy Reviews*, Volume 92, pp 1-8, 2018

[9] Tarighaleslami A.H., Ali Ghannadzadeh, Martin J. Atkins, Michael R.W. Walmsley, Environmental life cycle assessment for a cheese production plant towards sustainable energy transition: Natural gas to biomass vs. natural gas to geothermal, *Journal of Cleaner Production*, Volume 275, 2020, 122999

[10] Mabrouki J., Abbassi M.A., Khiari B., Jellali S., Zorpas A.A., Jeguirim M., The dairy biorefinery: Integrating treatment process for Tunisian cheese whey valorization, *Chemosphere*, Volume 293, 2022,133567

[11] Malliaroudaki M.J., Watson N.J., Ferrari R., Nchari L.N., Gomes R.L., Energy management for a net zero dairy supply chain under climate change, *Trends in Food Science & Technology*, 2022, in press
[12] Mainardis, M., Flaibani, S., Trigatti, M., Goi, D. Techno-economic feasibility of anaerobic digestion of cheese whey in small Italian dairies and effect of ultrasound pre-treatment on methane yield, *Journal of Environmental Management*, 246, pp. 557-563, 2019
[13] Romero A., M. Carvalho, D.L. Millar, Application of a polygeneration optimization technique for a hospital in Northern Ontario, *Trans. Can. Soc. Mech. Eng*., 38 (1) (2014), pp. 45-62
[14] Correia V.H.L, Portela de Abreu R., Carvalho M., Robustness within the optimal economic polygeneration system for a dairy industry, *Journal of Cleaner Production*, Volume 314, 2021, 127976
[15] Mančić M., Živković D., Djordjević M.L., Rajić M., Optimization of a polygeneration system for energy demands of a livestock farm, *Thermal Science*, 20(5), 1285-1300, 2016
[16] M.R. Chertow, Industrial symbiosis: literature and taxonomy, *Annu. Rev. Energy Environ*., 25 (1) (2000), pp. 313-337
[17] Afshari H., Babak Mohamadpour Tosarkani, Mohamad Y. Jaber, Cory Searcy,
The effect of environmental and social value objectives on optimal design in industrial energy symbiosis: A multi-objective approach, *Resources, Conservation and Recycling*, Volume 158, 2020, 104825
[18] Butturi MA, Lolli F, Sellitto MA, Balugani E, Gamberini R, Rimini B. Renewable energy in eco-industrial parks and urban-industrial symbiosis: A literature review and a conceptual synthesis. *Applied Energy*. 2019;255:113825
[19] Moser S, Lassacher S. External use of industrial waste heat - An analysis of existing implementations in Austria. *Journal of Cleaner Production*. 2020; 264:121531
[20] Lygnerud K, Werner S. Risk assessment of industrial excess heat recovery in district heating systems. *Energy*. 2018;151:430-441
[21] Kim H, Dong L, Earvin A, Choi S, Fujii M, Fujita T. Co-benefit potential of industrial and urban symbiosis using waste heat from industrial park in Ulsan , Korea. *Resources, Conservation and Recycling*. 2018;135:225-234
[22] Santin, M., Chinese, D., De Angelis, A., Biberacher, M., Feasibility limits of using low-grade industrial waste heat in symbiotic district heating and cooling networks, *Clean Technologies and Environmental Policy*, 22 (6), pp. 1339-1357, 2020
[23] Meneghetti, A., Chinese, D. Perspectives on facilities management for industrial districts, *Facilities*, 20 (10), pp. 337-348, 2002
[24] Best R., P. Rezazadeh Kalehbasti, Michael D. Lepech, A novel approach to district heating and cooling network design based on life cycle cost optimization, *Energy*, Volume 194, 2020, 116837
[25] Dominković D.F, Stunjek G., I. Blanco, H.Madsen, G. Krajačić, Technical, economic and environmental optimization of district heating expansion in an urban agglomeration, *Energy*, Volume 197, 2020

[26] Verena Halmschlager, Felix Birkelbach, Rene Hofmann, Optimizing the utilization of excess heat for district heating in a chipboard production plant, *Case Studies in Thermal Engineering*, Volume 25, 2021, 100900
[27] Keskin I., Soykan G., Optimal cost management of the CCHP based data center with district heating and district cooling integration in the presence of different energy tariffs, *Energy Conversion and Management*, Volume 254, 2022,115211
[28] Olsson L., Wetterlund E., Söderström M., Assessing the climate impact of district heating systems with combined heat and power production and industrial excess heat, *Resources, Conservation and Recycling*, Volume 96, 2015, Pages 31-39
[29] Bussieck M.R., Meeraus A. General Algebraic Modeling System (GAMS). In: Kallrath J. (eds) Modeling Languages in Mathematical Optimization. *Applied Optimization*, vol 88. Springer, Boston, MA, 2004.
[30] Chinese D., Optimal size and layout planning for district heating and cooling networks with distributed generation options, *International Journal of Energy Sector Management*, Vol. 2 No. 3, pp. 385-419, 2008.
[31] Chinese, D., Meneghetti, A., Nardin, G., Simeoni, P., From hospital to municipal cogeneration systems: An Italian case study, *International Journal of Energy Research*, 31 (9), pp. 829-848, 2007
[32] Retscreen International, *Retscreen online user manual – Solar air heating project model*, 2005
[33] Clark D.R., Klein S.A., Beckman W.A. Algorithm for evaluating the hourly radiation utilizability function. *ASME J. Solar Energy Engineering*, 105 (1983)
[11] Lazzarin, R.M. The importance of the modulation ratio in the boilers installed in refurbished buildings *Energy and Buildings*, 75, pp. 43-50, 2014
[12] Darrow K., Tidban R., Wang J., Hampson A., Catalog of CHP Technologies, US Environmental Protection Agency, 2017
[13] Torchio, M.F., Comparison of district heating CHP and distributed generation CHP with energy, environmental and economic criteria for Northern Italy, *Energy Conversion and Management*, 92, pp. 114-128, 2015
[14] Gopisetty, S., Treffinger, P., Generic combined heat and power (CHP) model for the concept phase of energy planning process, *Energies*, 10 (1), art. no. 11, 2017
[15] Ecoinvent, Lifecycle inventories of new CHP systems, 2007, available at https://db.ecoinvent.org/reports/20_SmallCombinedHeatPower.pdf?area=463ee7e58cbf8, last access 08.18.2021
[16] Umweltbundesamt Deutschland, Prozessorientierte Basisdaten für Umweltmanagementsysteme, https://www.probas.umweltbundesamt.de/php/index.php, last access 08.18.2021
[17] Lazzarin, R.M., Solar cooling: PV or thermal? A thermodynamic and economical analysis *International Journal of Refrigeration*, 39, pp. 38-47., 2014
[18] Greening, B., Azapagic, A. Domestic solar thermal water heating: A sustainable option for the UK?

(2014) *Renewable Energy*, 63, pp. 23-36.

[42] D'Antoni M., R. Fedrizzi, D. Romeli, Techno-Economic Analysis of Air-to-Water Heat Rejection Systems, *Proceedings Eurosun* 2014, Aix-les-Bains, France, 2014, http://proceedings.ises.org/paper/eurosun2014/eurosun2014-0074-DAntoni.pdf

[43] ARERA, https://www.arera.it/it/portaleofferte.htm, Last access 08.18.2021

[44] ISPRA, Fattori di emissione atmosferica di gas a effetto serra nel settore elettrico nazionale, 2020 Edition https://www.isprambiente.gov.it/files2021/pubblicazioni/rapporti/r343-2021.pdf, 2021

[45] Cplex II. V12. 1: User's Manual for CPLEX. International Business Machines Corporation. 2009;46(53):157.